The L'Aquila 2009 event: the GPS deformations

L. Biagi[1], S. Caldera[1], D. Dominici[2] and F. Sansò[1]

[1] *Politecnico di Milano, Como, Italy*
[2] *Università de L'Aquila, L'Aquila, Italy*

ABSTRACT   In the night of April 6, 2009, an earthquake of M_W 6.3 magnitude occurred in the Abruzzo region. The hypocenter was estimated by the INGV at 42,35° N, 13,38° E, at a 9.5 km depth; moreover, at least one month of pre-seismic events preceded the main shock and aftershocks continued for at least 6 months. For the understanding of the geodetic and geodynamic implications of the earthquake, the temporal and spatial analyses of the phenomenon are fundamental; our research group has collected the GNSS data provided by about 50 permanent stations in the earthquake area and neighbouring regions; all the data have been processed in order to investigate the stations displacements and, if possible, the deformation pattern. In particular, the time series (two months of data both before and after the earthquake) of the daily coordinates were interpolated for each station in order to estimate the displacement at the main shock epoch: particular attention has been paid to carry out a proper covariance empirical estimation, in order to evaluate the displacement significance. Finally, the displacements of all the stations have been spatially analyzed to indentify the areas with similar displacements and the main discontinuities between them. Thirteen stations that significantly displace horizontally have been found: a rough clustering allows us to discriminate between a near field area that displaces mainly southwards, a south-western region that displaces in a SWdirection and a northeast region with an opposite motion. Only four station in the epicenter area significantly displace vertically, with drops between 3 and 12 cm.

1. Introduction

The L'Aquila event is identified here by the main shock of the Abruzzo earthquake, which took place on April 6, 2010 at 1.33 UTC, with a magnitude of M_W 6.3 (Anzidei *et al.*, 2009; EMERGEO Working Group, 2009; INGV, 2009); this was preceded by foreshocks and followed by aftershocks. The event was catastrophic, as it could only be, considering that the epicenter (42,35° N, 13,38° E, depth of 9.5 km) is placed in the middle of a populated area, with historical buildings, inadequate to withstand such strong dynamics. Scientists are analyzing the existing data to take one step forward along the hard road of understanding the physics and predicting such phenomena. The data that allow us to reconstruct the displacements and the deformation pattern of the Earth's surface in the earthquake area are of great importance, because they can provide input information for geophysical analyses and inversions (Okada, 1985): nowadays they are mainly of two types, referring to the GNSS and inSAR techniques. The latter is stuck in time to the repeat cycle of SAR satellites ($\approx$ 35 days), meaning that the deformation story is somewhat forcedly discontinuous in time. On the other hand SAR, in both its versions, interferometric

(Hanssen, 2001) and Permanent Scatterers (Ferretti *et al.*, 2001), is capable of providing a real area-wise picture of the deformation pattern. On the other hand, data acquired by permanent GNSS stations (PS's) are almost continuous in time (typically up to 1 Hz rate, though in this paper the 30 s acquisition interval has been analyzed), their disadvantages being related to their sparseness in the area and to the fact that, when placed on the roof of a building, they describe the kinematics of the building coupled through foundations with the ground, rather than the direct displacement of the ground itself. A combined analysis of data for both techniques is obviously the optimal solution for an accurate reconstruction of the deformation story: yet, in the present work we present the image of the ground motion derived from GNSS data only.

Only in the Abruzzo region, we can collect data from 33 PS's: in particular, five of them are less than 10 km away from the epicenter; moreover, we have another 17 additional PS's within 50 km from the region's boundaries and the three nearest Italian IGS stations of Matera, Cagliari and Medicina have been included, to provide a proper link to ITRS. All the stations already belong to some permanent network: ASI-Geodaf, (geodaf.mt.asi.it, Vespe *et al.*, 2000), INGV-RING (ring.gm.ingv.it, Avallone *et al.*, 2010), Leica ItalPoS (www.italpos.it), TopCon GeoTop (www.geotop.it), GPS Abruzzo (gpsnet.regione.abruzzo.it), GPS Umbria (opos6.agora.ng.unipg.it), ResNap (w3.uniroma1.it/resnap-gps); the authors want to gratefully acknowledge these organizations for providing the data.

This relative abundance of data allows a sufficient reconstruction of the deformation field with a spatial resolution of about 10 km, particularly in the epicenter area, and a time resolution of 30 s; note that the spatial consistency of the estimated displacements of different stations should confirm that we are not seeing the motion of the individual structures. In Sect. 2, we present the data used in the work, and outline the analysis strategy. In Sect. 3, we perform the analysis of the time series of the displacements, in a local (east, north, up) coordinate system of the individual stations. In Sect. 4, we make some considerations on the deformation pattern and its spatial discontinuities, both in the plane and in the vertical direction. Provisory conclusions and outlooks of future work are presented in Sect. 5.

2. The data set and processing strategy

The data used in this work are the daily (with a 30 s acquisition interval) RINEX files of all the PS's listed in the previous section. The data have been processed by daily adjustments of the network from Sunday February 1 (Day Of the Year 32, GPS Week 1517, day of the GPSW 0) to Saturday June 6 (DOY 157, GPSW 1534, DOW 6), namely 64 days before the event and 61 days after the event: in this way, two months of results are available both before and after the main shock.

Ancillary data for the processing were the final IGS products for ephemerides, Earth orientation parameters and phase center variations. The network adjustment has been performed by the Bernese 5.0 software [BSW5.0, Dach *et al.* (2007)]; in the design of the multibase graph the minimum baseline length principle has been adopted; in the raw data processing the approach described in Benciolini *et al.* (2008) and the usual international guidelines (Kouba, 2003) have been followed. To remove the intrinsic rank deficiency of this local network, minimal constraints have been imposed to each daily solution, by fixing the 3 translation parameters to the barycenter
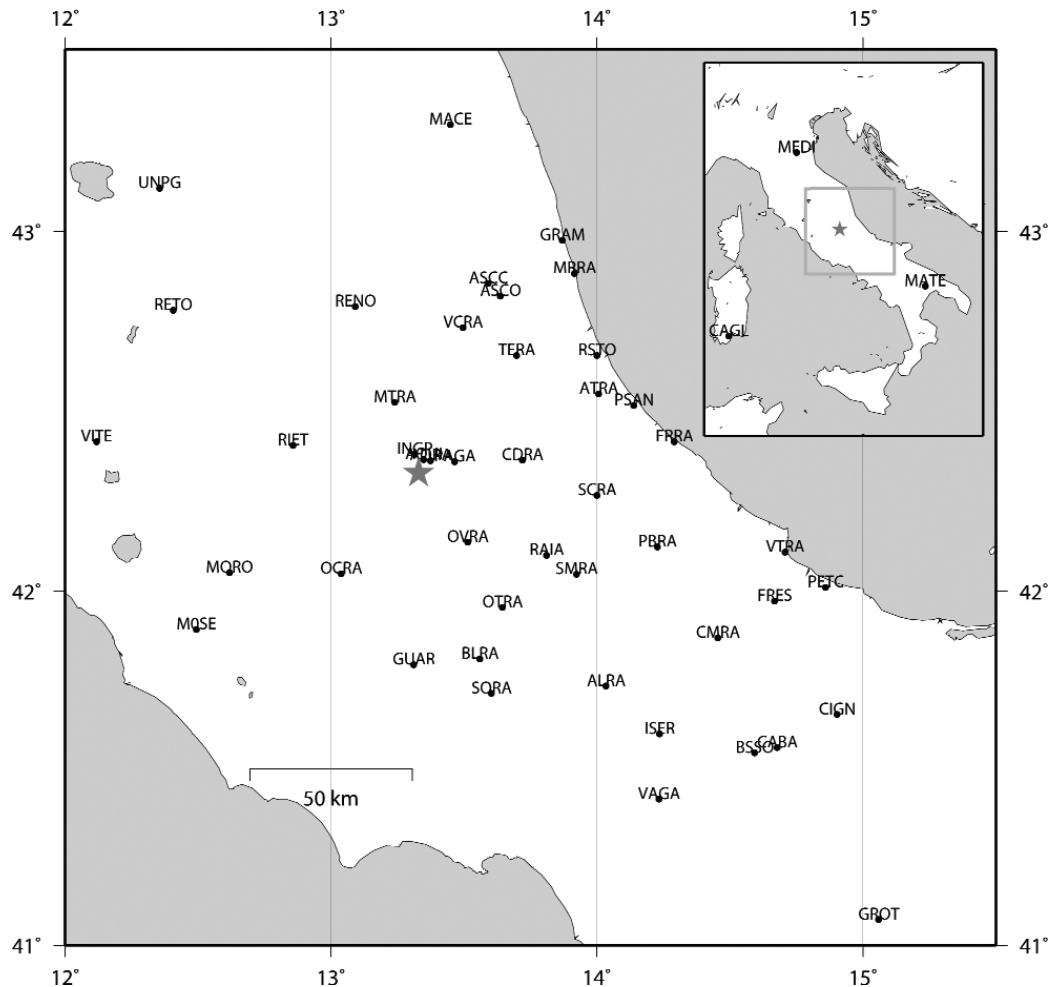
Fig. 1 - The GNSS Permanent Network analyzed in the present paper. Upper box: the IGS reference stations; main map: the final configuration (after outliers rejection) of the local network. Gray star: earthquake epicenter.

of the a priori coordinates of the IGS PS's; these have been computed by interpolating the previous 52 weekly IGS solutions, in the IGS05 reference frame (Ferland *et al*., 2004; Ferland, 2006; Altamimi *et al*., 2007; the relevant documentation is continuously updated on the IGS website: //igscb.jpl.nasa.gov/). In the data processing, a severe rejection has been applied, in order to remove

    1. stations with significant data gaps,

    2. twin stations in the same area (clearly with the exception of the stations near the epicenter),

    3. stations whose time series of daily coordinates showed a large noise.

From the 61 available, 12 stations have been excluded: therefore, the final network (Fig. 1) is composed of 49 stations, of which four (AQUI and AQRA in L'Aquila, INGP in Preturo, PAGA in Paganica) are in the near field of the main shock epicenter. Before analyzing the time series and the main shock discontinuities, we want to underline an anomalous behaviour which is
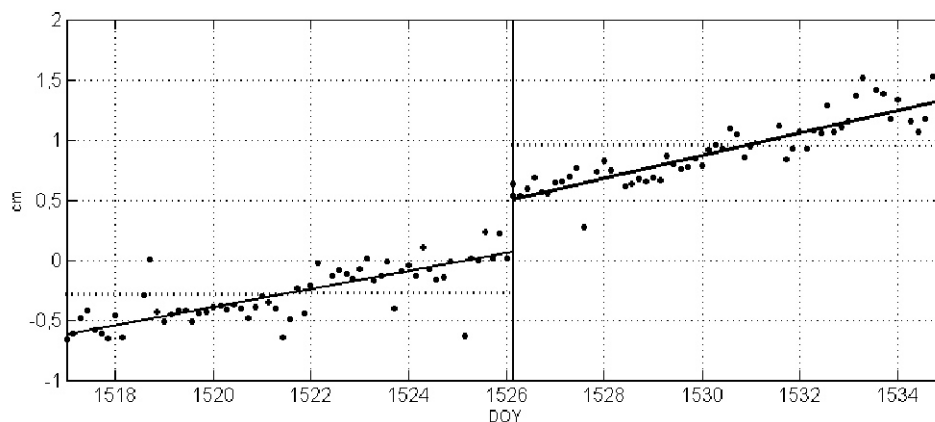
Fig. 2 - Example of different estimates of the jump provided by different time models for the time series before and after the event; the ASCO (Ascoli) north component example. Linear interpolation: continuous line. Mean position: dotted line.

present in several daily solutions of week 1521, well before the earthquake (see the example in the following Figs. 3, 4, 5 and 6); probably the anomalous results are caused by some irregularity in the adjustment and seem totally independent of the geophysical event we want to analyze: indeed, they are common both to the IGS and local PS's, irrespective of their position, and do not show a clear temporal signal.

3. The individual displacements of the stations

The first analysis concerns the time series of the daily coordinates of each station. At first, the daily estimated coordinates of the three IGS stations were compared with their a priori values, in order to assess the reference frame accuracy and stability: the statistics (Table 1) are completely satisfying, showing standard deviations of about 2 mm in the local horizontal components and 4 mm in height.

Our first purpose is to estimate the pattern of the time evolution of the coordinates before and after the main shock, trying then to reconstruct the amplitude of the relevant discontinuity. The

Table 1 - Statistics of the residuals of the daily estimates with respect to the a priori coordinates for the IGS stations. E: mean value; σ: standard deviation; Min: minimum; Max: maximum.

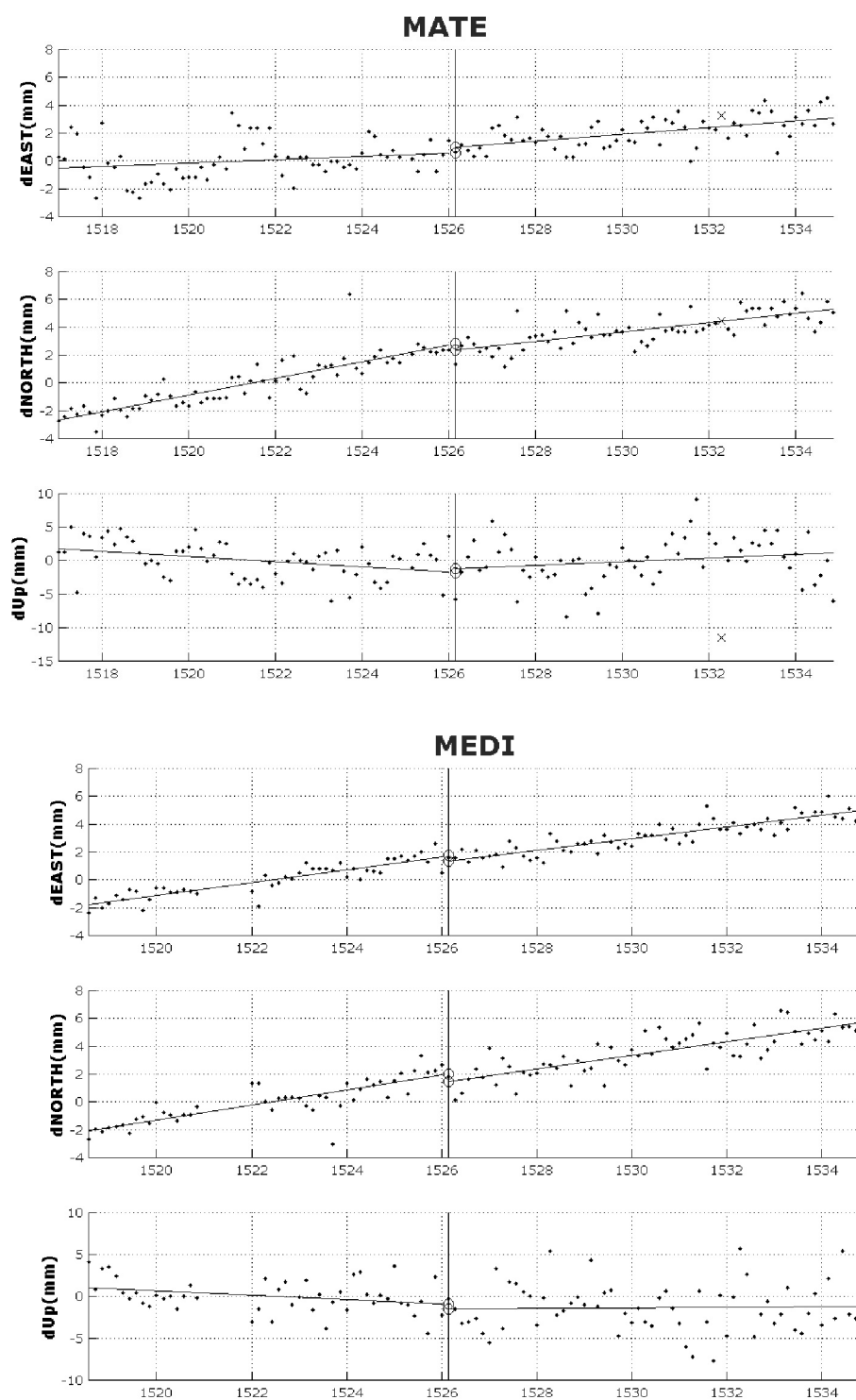| (mm)	East	North	Height
E	0.6	0.4	0.5
σ	2.7	1.0	4.1
Min	-4.0	-2.6	-10.8
Max	6.4	6.6	17.4

Fig. 3 - Example of time series (with respect to the mean coordinates) for stations far from the earthquake epicenter: MATE and MEDI. Note the anomalous results of MATE in week 1521. Dots and crosses represent the accepted and the rejected daily solutions respectively; lines are the resulting linear interpolations before and after the earthquake.

interpolation of the time series can be easily accomplished by Least Squares [LS: see, for example, Koch (1987)]; in this regard, the choice of the model to interpolate the time series of the daily solutions before and after the earthquake is of an overlay importance. Generally, to interpolate long time series, the adoption of the linear model [Eq. (1)] is suggested. However, for data sets that span a few months, the typical praxis is to simply estimate the mean coordinates: indeed, the estimated velocities are not significant from a geophysical point of view and contain also the effects of seasonal effects (Blewitt and Lavallèe, 2002; Ray *et al.*, 2008). In our case, the simple computation of the mean coordinates could produce an estimate of the main shock discontinuity dramatically different from that provided by the linear model; an example is given by the north coordinate of the ASCO station (Fig. 2): the difference between the mean coordinates before and after the main shock is of 13 mm, while the discontinuity estimated by the adoption of two linear models is just of 5 mm and is clearly more realistic. So, despite the shortness of our data set, in order to improve the estimates of the discontinuities at the main shock epoch, we have decided to use the complete linear model.

Estimated discontinuities should always be accomplished by their covariance matrices in order to rigorously understand which points have really significantly displaced; this is not an easy task, because in GNSS data processing, the space and time stochastic model of the residuals is usually over simplified, resulting in a strong underestimation of the variance of the daily coordinates of the adjusted stations (Barzaghi *et al.*, 2004): it is well known that LS solutions tend to underestimate the variances of the parameters, when the prior covariance model of the observations is not correctly provided. So, in our test, some empirical estimation of the covariance should be performed.

Generally, a joint estimation of the parameters and of the stochastic model involves simplified assumptions and typically is performed by iterative approaches. In our case, we assume that the covariance matrix of the daily network solutions is the same every day and that the network solutions of different days are not correlated: under these hypotheses, in Biagi and Dermanis (2006) it is proved that a closed solution for both parameters and covariances can be computed without iterations; the approach is briefly summarized here. Let us call $\boldsymbol{\eta}_{kj}$ the vector of the D coordinates of station k derived by the network adjustment at day t_i: $D=3$ in the case of a complete three dimensional analysis, $D=2$ in the case of a pure horizontal analysis; let us define T the number of days and S the number of stations. The vectors $\boldsymbol{\eta}_{kj}$ satisfy a linear model in time and have a covariance structure, inherited from the GPS observations, which according to our hypotheses can be written as

$$\boldsymbol{\eta}_{k,i} = \overline{\boldsymbol{\eta}}_k + (t_i - \overline{t})\dot{\boldsymbol{\eta}}_k + \mathbf{v}_{k,i}, \ E\{\mathbf{v}_{k,i}\mathbf{v}_{l,j}^T\} = \delta_{ij}\boldsymbol{\Sigma}_{kl} \tag{1}$$

where i,j are time indexes, k,l are station indexes, $\overline{t}$ and $\overline{\boldsymbol{\eta}}$ are respectively some reference epoch and the relevant coordinates: a typical choice is to put $\overline{t}$ equal to the mean epoch of the interpolated data; $\dot{\boldsymbol{\eta}}$ is the velocity. The daily observations can be further put in vectors $\boldsymbol{\eta}_i$ that include all the coordinates of the PS's at day t_i:
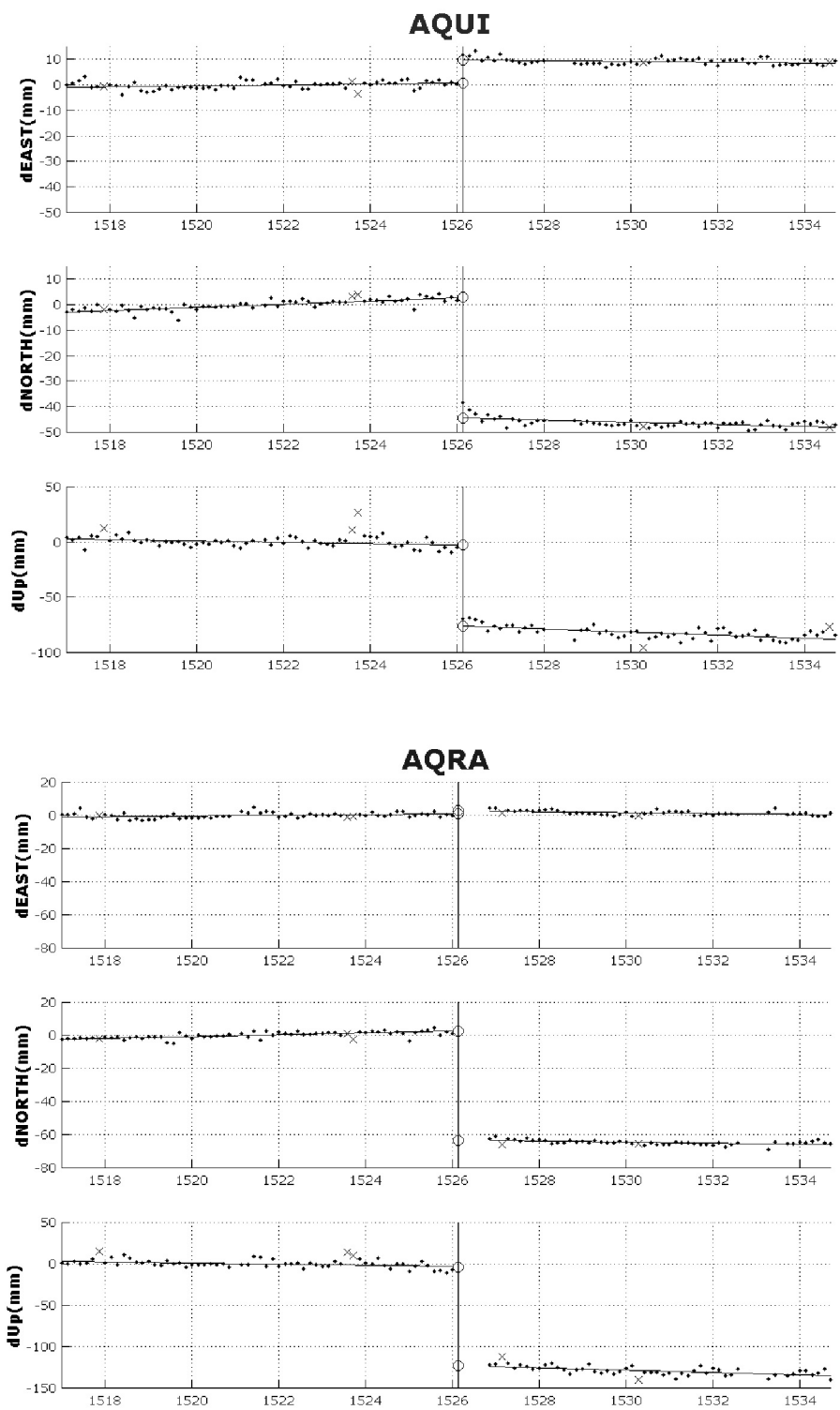
Fig. 4 - Daily time series and relevant interpolations of AQUI and AQRA. Dots and crosses represent the accepted and the rejected daily solutions respectively; lines are the resulting linear interpolations before and after the earthquake.

$$\boldsymbol{\eta}_i = \begin{bmatrix} \boldsymbol{\eta}_{1,i} \\ ... \\ \boldsymbol{\eta}_{S,i} \end{bmatrix}, \qquad \boldsymbol{\Sigma}_{n_i n_i} = \boldsymbol{\Sigma} = \begin{bmatrix} \boldsymbol{\Sigma}_{11} & \boldsymbol{\Sigma}_{21} & ... & \boldsymbol{\Sigma}_{S1} \\ \boldsymbol{\Sigma}_{12} & \boldsymbol{\Sigma}_{22} & ... & \boldsymbol{\Sigma}_{S2} \\ ... & ... & ... & ... \\ \boldsymbol{\Sigma}_{1S} & \boldsymbol{\Sigma}_{2S} & ... & \boldsymbol{\Sigma}_{SS} \end{bmatrix} \tag{2}$$

We then collect all the observations, their covariance and the unknowns:

$$\mathbf{y} = \begin{bmatrix} \boldsymbol{\eta}_1 \\ ... \\ \boldsymbol{\eta}_S \end{bmatrix}, \quad \mathbf{C}_{yy} = \mathbf{I}_{T \times T} \otimes \boldsymbol{\Sigma}; \quad \overline{\boldsymbol{\eta}} = \begin{bmatrix} \overline{\boldsymbol{\eta}}_1 \\ ... \\ \overline{\boldsymbol{\eta}}_S \end{bmatrix}, \quad \dot{\boldsymbol{\eta}} = \begin{bmatrix} \dot{\boldsymbol{\eta}}_1 \\ ... \\ \dot{\boldsymbol{\eta}}_S \end{bmatrix}, \quad \mathbf{x} = \begin{bmatrix} \overline{\boldsymbol{\eta}} \\ \dot{\boldsymbol{\eta}} \end{bmatrix} \tag{3}$$

The parameters and the network covariance can be then estimated by LS:

$$\hat{\mathbf{x}} = \begin{bmatrix} \hat{\overline{\boldsymbol{\eta}}} \\ \hat{\dot{\boldsymbol{\eta}}} \end{bmatrix} = (\mathbf{R}^T \mathbf{R})^{-1} \mathbf{R}^T \otimes \mathbf{I}_{DS \times DS} \mathbf{y} \quad \hat{\boldsymbol{\Sigma}} = \frac{1}{T-2} \sum_{i=1}^{T} \hat{\mathbf{v}}_{ti} \hat{\mathbf{v}}_{ti}^T \tag{4}$$

where

$$\mathbf{R} = \begin{bmatrix} 1 & t_1 \\ ... & ... \\ 1 & t_T \end{bmatrix} \tag{5}$$

$\mathbf{v} = \boldsymbol{\eta}_i - \hat{\boldsymbol{\eta}}_i$ are the daily residuals for day t_i and $\hat{\boldsymbol{\eta}}_i$ are the LS estimates of the daily coordinates of the network. Note that the parameter estimates do not depend on the network covariance matrix; moreover, they are equal to the estimates obtained by a simple linear regression of the individual coordinates; finally, $\boldsymbol{\Sigma}$ can be empirically computed and the covariance matrix of $\hat{\mathbf{x}}$ can be estimated by

$$\mathbf{C}_{\hat{x}\hat{x}} = (\mathbf{R}^T \mathbf{R})^{-1} \otimes \hat{\boldsymbol{\Sigma}}^{-1} \tag{6}$$

Given a station *k*, its coordinates and the relevant covariance at the main shock epoch *e* are given by

$$\hat{\boldsymbol{\eta}}_{k,e} = \hat{\overline{\boldsymbol{\eta}}}_k + (t_e - \overline{t})\hat{\dot{\boldsymbol{\eta}}}_k, \quad \mathbf{C}_{k,e} = \mathbf{C}_{\overline{\eta},\overline{\eta}} + (t_e - \overline{t})^2 \mathbf{C}_{\dot{\eta},\dot{\eta}} + 2(t_e - \overline{t})\mathbf{C}_{\overline{\eta},\dot{\eta}}. \tag{7}$$
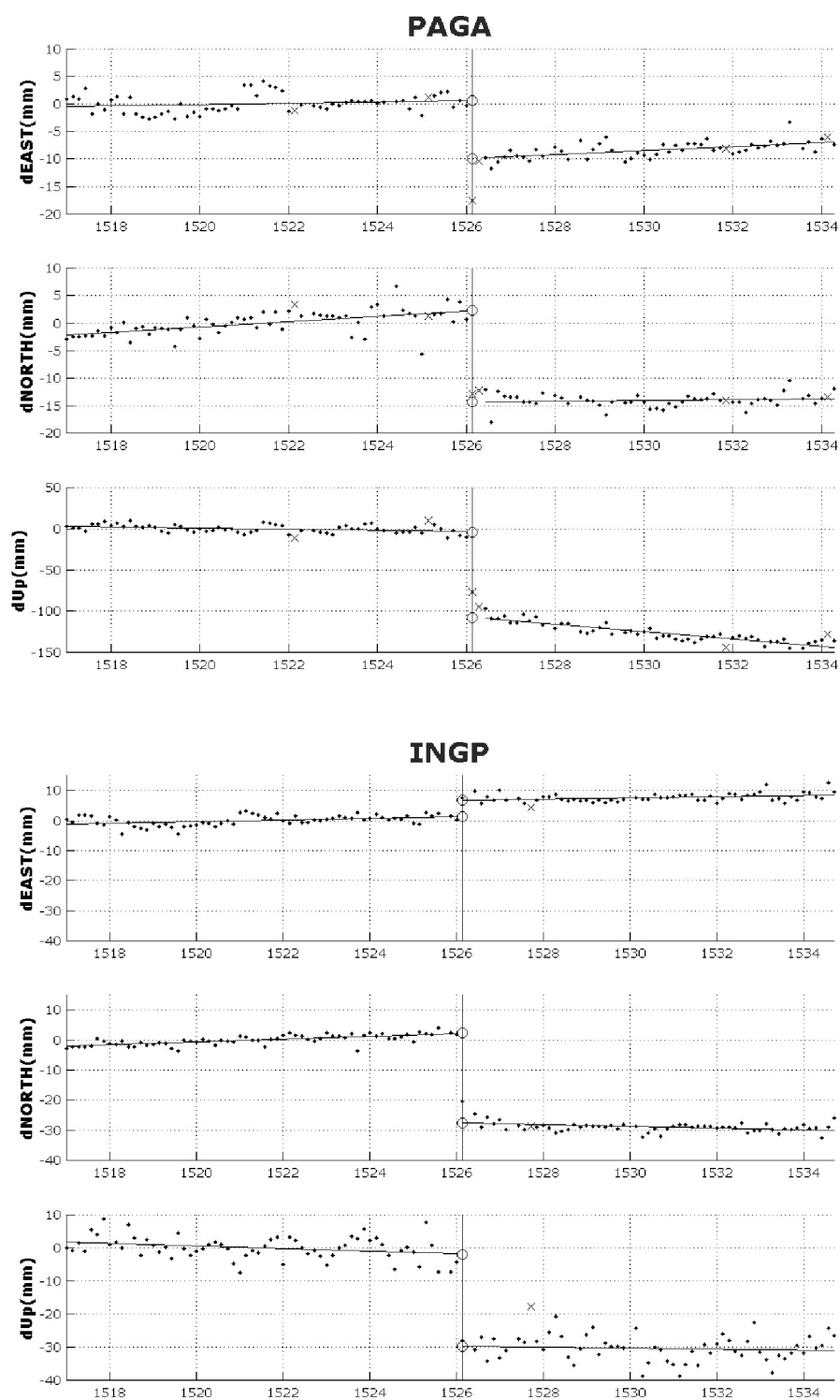
PAGA

INGP

Fig. 5 - Daily time series and relevant interpolations of PAGA and INGP. Dots and crosses represent the accepted and the rejected daily solutions respectively; lines are the resulting linear interpolations before and after the earthquake.

Table 2 - Statistics of the residuals of the daily estimates with respect to the linear models. E: mean value; σ: standard deviation; Min: minimum; Max: maximum.

Before Earthquake				After Earthquake			
(mm)	**East**	**North**	**Height**	**(mm)**	**East**	**North**	**Height**
E	0.0	0.0	0.0	E	0.0	0.0	0.0
σ	1.5	1.3	3.6	σ	1.1	1.2	3.9
Min	-6.1	-6.3	-11.1	Min	-6.9	-6.9	-9.9
Max	7.1	5.9	11.4	Max	7.8	7.7	11.6

In our application, for each station, two estimates of Eq. (7) exist: the first for the forward prediction from pre-event time series, the other for the backward prediction from the post-event time series: we call them respectively η^-_k , C^-_k and η^+_k , C^+_k. We can define the discontinuity vector and its covariance

$$\delta\,\boldsymbol{\eta}_k = \hat{\boldsymbol{\eta}}^+_{e,k} - \hat{\boldsymbol{\eta}}^-_{e,k}\quad \mathbf{C}_{\delta\delta} = \mathbf{C}^+_k + \mathbf{C}^-_k.$$
(8)

At this point the standard test on the hypothesis $H_0 : \mathrm{E}\{\delta\,\hat{\boldsymbol{\eta}}_k\}=0$ is

$$\{\delta\hat{\boldsymbol{\eta}}^T_k \mathbf{C}^{-1}_{\delta\delta}\delta\hat{\boldsymbol{\eta}}_k\} = \hat{\chi}^2 \leq \chi^2_{2,\alpha} \Rightarrow H_O \quad accepted$$
(9)

where $\chi^2_{2\alpha}$ is the initial value of a χ^2 with 2 degrees of freedom and significance level equal to α.

Before the significance analysis of the discontinuities, the general behaviour of the results is briefly discussed. The time series and the relevant interpolations of all the 49 stations involved in the adjustment have been published on the server of the Geomatics Laboratory of the Politecnico di Milano (Biagi *et al*., 2010); there, we will concentrate on some typical behaviour, particularly for the four stations in the focal area and for two stations far away, about 40-45 km from the epicenter but in opposite directions (TERA in Teramo, OCRA in Oricola).

Once the outliers have been removed, the statistics of the daily results (Table 2) are quite satisfactory; three stations in the focal area present a larger variability of the daily residuals after the event: this could be due to the post seismic settlement of the area after the main shock.

In some cases, the linear behaviour of the time series of the coordinates has a sudden discontinuity at the event, but then it continues basically with the same velocity as before; for other stations, the velocity apparently changes at the event (Fig. 5, Up component of PAGA); in any case, an analysis of the velocity changes based on the time series of a few months is not meaningful because they can be caused also by seasonal effects: this is a good reason to describe the deformation field essentially through an instantaneous field at the event, to which the ordinary linear ground motion is superimposed. In particular, for the stations near the epicenter, one might expect a typical exponential post-seismic relaxation: actually, an inspection of the
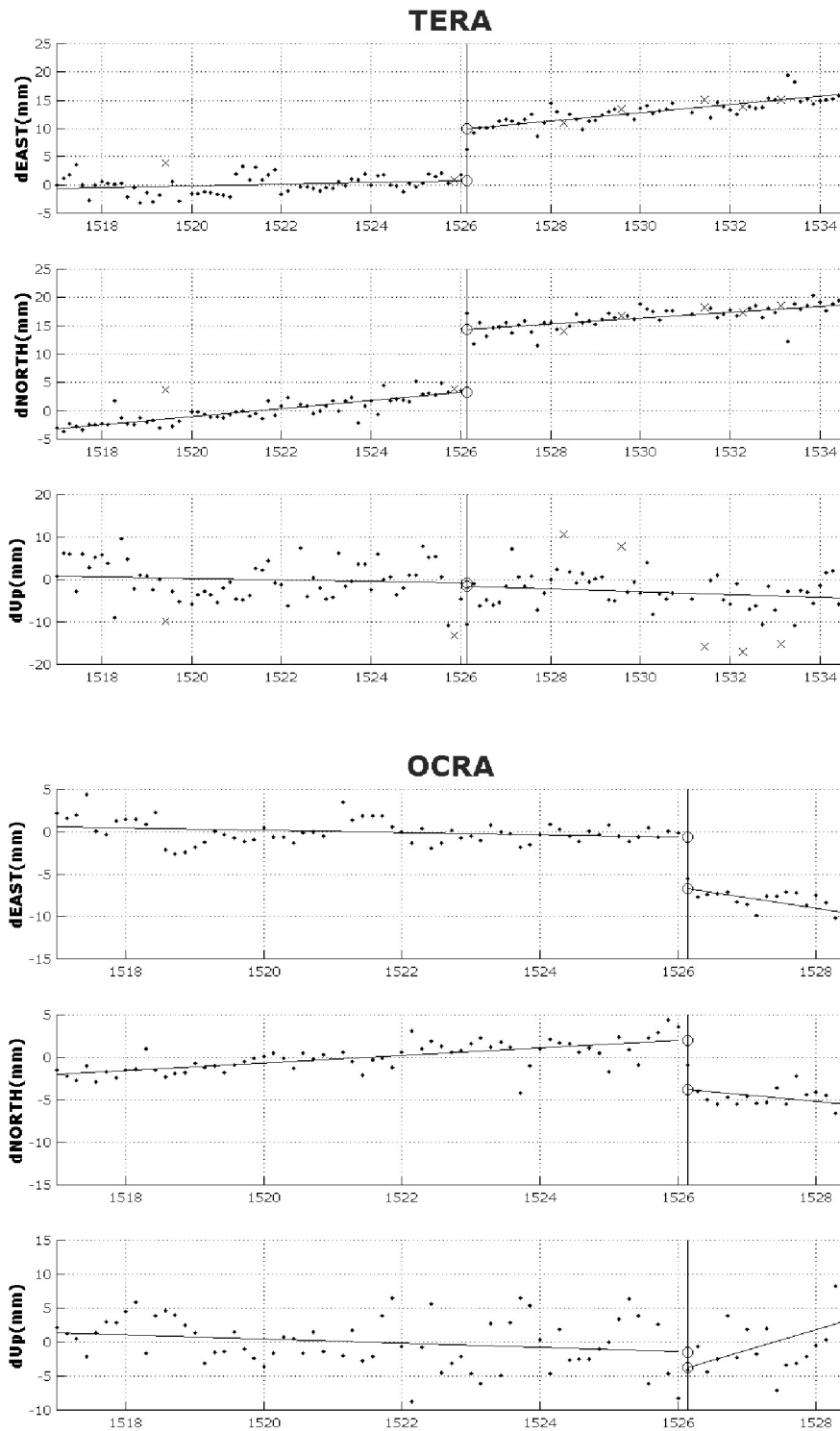
Fig. 6 - Daily time series and relevant interpolations of TERA and OCRA. Dots and crosses represent the accepted and the rejected daily solutions respectively; lines are the resulting linear interpolations before and after the earthquake. Unfortunately the OCRA time series is interrupted three weeks after the event: nevertheless the discontinuity is well visible.
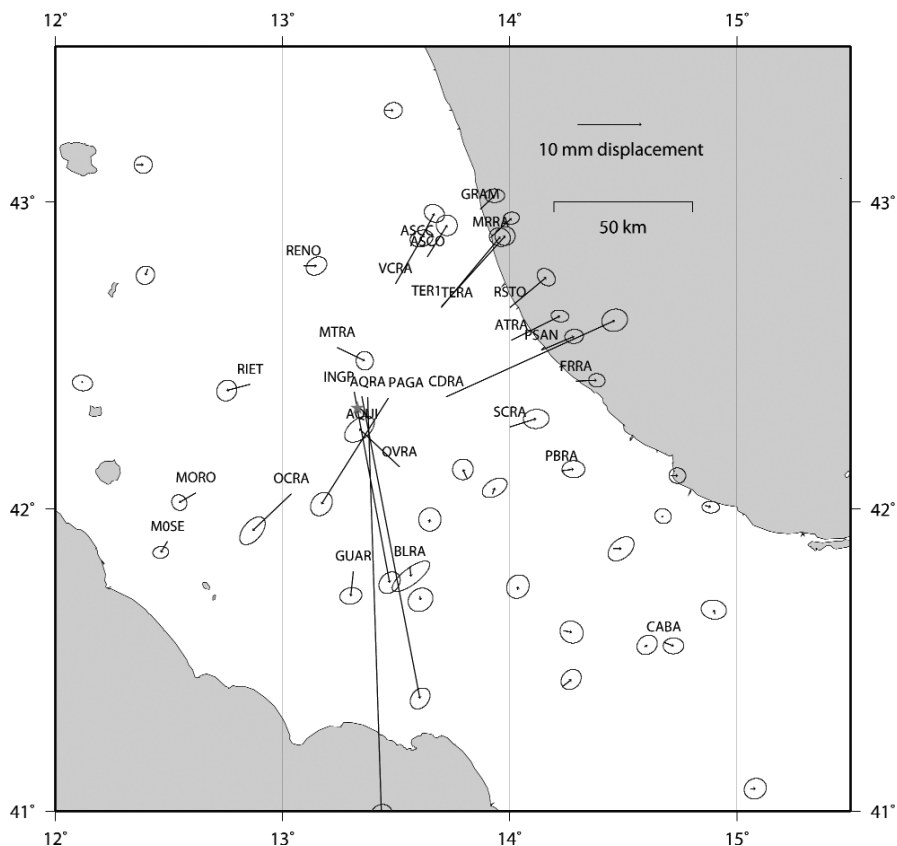
Fig. 7 - Horizontal displacements of the local network stations. The gray ellipses depict the 99% confidence regions of the vectors; the dotted segment roughly highlights the main discontinuity line in the horizontal displacements field. The names of the stations that significantly displace are reported.

residuals of the linear interpolation reveals that this phenomenon is present in two stations of the epicentral area. In AQUI (Fig. 4), an exponential behaviour appears in the north component, with an amplitude of about 6 mm and a time constant of 1~2 days; some relaxation, but not a clear exponential signal, could be present in the Up component. In PAGA (Fig. 5), the Up shows a clear exponential, with amplitude of 10 mm and time constant of 2 days; the east component shows a residual of 8 mm the first day after the main shock, but not a correlated pattern for the following days; the north residuals are correlated, but do not show an exponential behaviour. The other two sites near the epicenter (AQRA and INGP) show irregularities but not a clear relaxation. The rigorous analysis of long term relaxations requires the separation between any possible seasonal effect, a long term exponential and the linear trend: it will be possible when time series longer than one year after the event are available.

In the following discontinuity analysis, we have decided to separate the horizontal and the vertical analysis, because their spatial behaviours are very different (compare Figs. 7 and 8). As the horizontal discontinuities are concerned, the stations that significantly displace, and the relevant displacements, are reported in Table 3. A totally equivalent, but graphically more
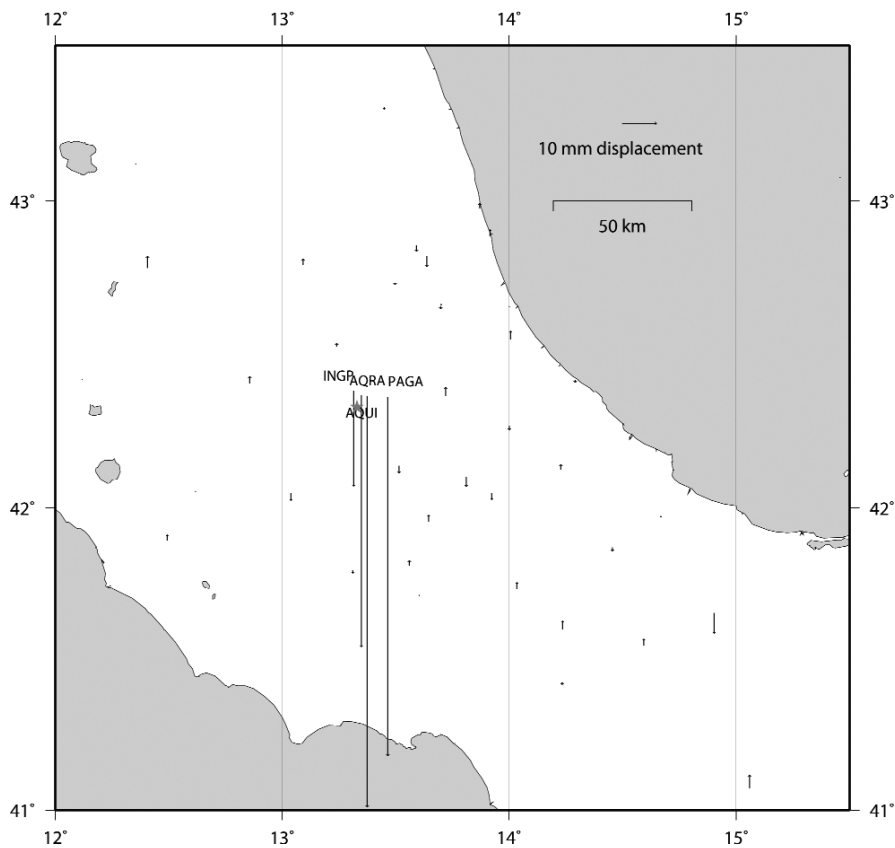
Fig. 8 - Vertical displacements of the stations. The only significant displacements are the largest four near the epicenter: the names of the relevant stations are reported.

Table 3 - List of the stations that significantly displace (significance level $\alpha=1\%$), relevant horizontal displacements in mm and empirical chi squared. The list is ordered (from top to bottom, from left to right) in order of displacement magnitude.

| Station	φ(° N)	λ(° E)	δE	δN	χ^2	Station	φ(° N)	λ(° E)	δE	δN	χ^2
AQRA	13.3743	42.3659	2	-66	78	ASCO	13.6369	42.8225	3	5	73
AQUI	13.3502	42.3682	9	-47	92	MTRA	13.2400	42.5278	4	-2	7
INGP	13.3156	42.3825	6	-30	48	OCRA	13.0390	42.0495	-6	-6	9
CDRA	13.7201	42.3675	26	12	29	GUAR	13.3122	41.7944	-1	-4	19
PAGA	13.4656	42.3623	-10	-17	132	MORO	12.6190	42.0525	-3	-1	17
TERA	13.6981	42.6571	9	11	36	FRRA	14.2922	42.4178	3	0	11
TER1	13.7004	42.6621	10	11	49	GRAM	13.8705	42.9755	2	2	8
ATRA	14.0073	42.5515	8	4	35	RIET	12.8571	42.4076	-4	-1	3
RSTO	14.0015	42.6584	6	5	19	SCRA	14.0021	42.2681	4	1	12
VCRA	13.4975	42.7354	4	7	21	M0SE	12.4933	41.8931	-1	-2	8
OVRA	13.5151	42.1376	-6	6	19	RENO	13.0931	42.7928	2	0	7
ASCC	13.5930	42.8573	3	5	8	BLRA	13.5603	41.8103	0	-1	6
PSAN	14.1390	42.5188	5	2	19	PBRA	14.2285	42.1242	2	0	21
MRRA	13.9160	42.8853	3	3	15	CABA	14.6784	41.5604	1	-1	46
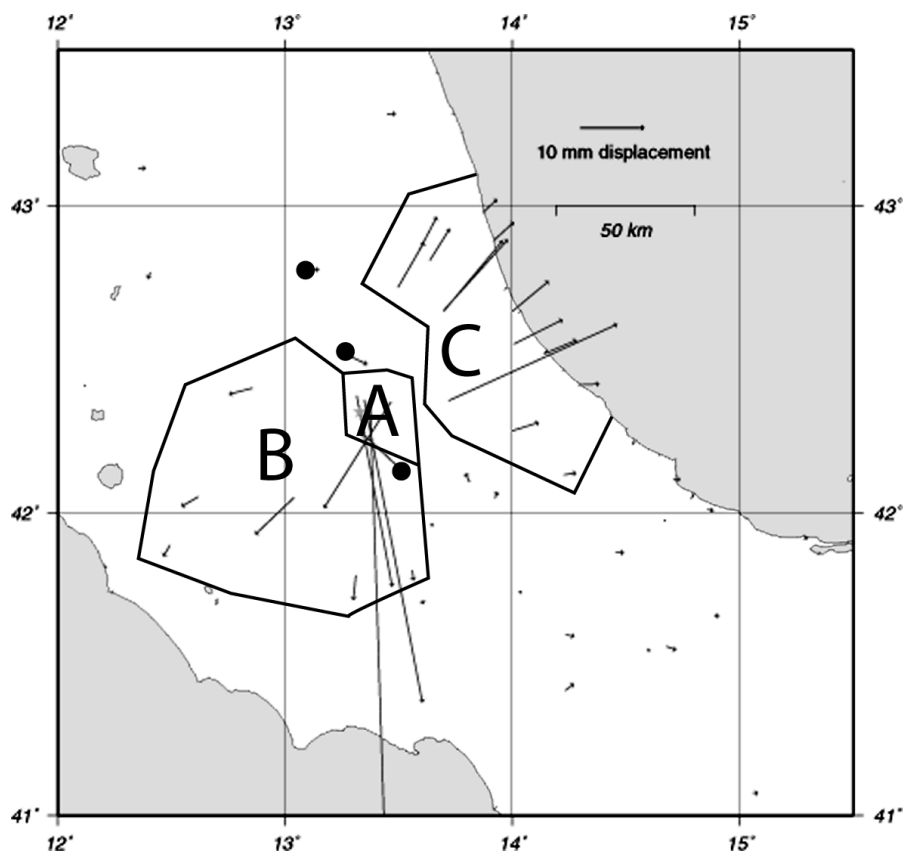
Fig. 9 - Clustering of the stations significantly displaced into homogeneous horizontal behaviours. In the middle, the stations in the epicenter area jump almost homogeneously in a south direction (A region); the B region displaces towards SW; the C region shows homogeneous displacements towards NE; the three significant but not consistent movements are marked with a circle; the other displacements are not significant.

readable representation of the test of Eq. (9), is to draw the confidence region around the observed discontinuity $\delta\hat{\eta}_k$, behaving a probability $1-\alpha$; when this region includes the origin of $\delta\hat{\eta}_k$, the jump is not significant, otherwise it is: the results can be seen in Fig. 7. The signature of the displacements near the epicenter is quite clear: PAGA moves SW, while the other three stations are displaced basically southwards. If we move from the epicenter for about 40 km SW, we find, for instance, OCRA while at a slightly larger distance northeast, 47 km, we meet TERA. These two stations have a nicely opposite behaviour: OCRA moves by about 0.9 cm SW while TERA moves about 1.5 cm NE (Fig. 6). This behaviour seems to be quite systematic, and we can draw a line across which the horizontal displacement field undergoes a sharp discontinuity (Figs. 7 and 9); just two stations show different motion trends with respect to the surrounding ones; the first is about 25 km north from the epicenter (MTRA), the second (OVRA) is at the same distance in the south direction. Of course there is no pretence of accuracy in the design of the above segment, yet we observe that its direction and position appear to be consistent with the faulting system in the area (Serpelloni *et al.*, 2005; Anzidei *et al.*, 2009).

A rigorous significance analysis could be repeated for the displacements in the vertical discontinuities; in any case, as Fig. 8 clearly shows, the visual analysis by itself allows us to identify the four stations, all those near the epicenter, that significantly displace in the Up component: INGP (-2.7 cm), AQUI (-7.3 cm), PAGA (-10.4 cm) and AQRA (-11.9 cm); no other significant vertical motions occur, with a range between -3 mm and 3 mm.

4. Spatial analysis of the displacements

The object of this section is the spatial analysis of the instantaneous displacement field, as reconstructed from the discontinuities in the individual time series.

The ground displacements (Fig. 7) clearly show a discontinuous behaviour and not a spatial smooth pattern: a preliminary cluster analysis is required to define at least the subregions with a consistent internal pattern. In this way, as far the horizontal displacements (with the exception of MTRA and OVRA, mentioned in Sect. 3, and RENO, less evident) we have found 3 main subregions that could be characterized in the following way (Fig. 8):

- the focal region (A region), where three stations (AQRA, AQUI and INGP) show an intense motion towards south (20-70 mm), one station (PAGA) experiences a SW motion of about 20 mm;
- the SW region (B region), where at least 6 stations experience a moderate but significant SW motion (up to 30 mm); only OVRA displaces toward NW, by about 9 mm;
- the NE region (C region), where at least 14 stations experience a moderate but significant NE motion (up to 30 mm).

The results are similar to those found by Anzidei *et al*. (2009), Atzori *et al*. (2009) and Cheloni *et al*. (2010); in particular, in their works, detailed discussions and geophysical interpretations of the dynamics in the near field A region are provided.

In both B and C subregions, the number of stations is always too small to allow a consistent prediction of the inner displacement field, based on the analysis of the spatial covariance. One remark is that apparently the diameter of the B region is smaller than that of the C region, which is reaching the sea and where the jump vector undergoes a rotation from NE to E while we move the application point from north to south. From Fig. 9, we see clearly that outside the region of significant movements, there is a belt where the displacement vectors are still coherent as for their directions, although the amplitude of the vector is too small to be significant. In any case, our results confirm the already known (see for example: D'Agostino *et al*., 2008; Devoti *et al*., 2008) SW-NE extension phenomena that interest the Apennines. As far the vertical movements are concerned, no real clustering is possible because in front of a very intense fall of the stations in the focal area no significant vertical motions can be found anywhere else.

5. Conclusions

A first conclusion can be drawn on the kinematics of the event; in particular, our results are summarized in the following 4 points.

1. The most intense displacement is a vertical fall of the focal area of about 10 cm; no other significant vertical motion is present.

2. This is accompanied by a movement, mainly to the south of the four stations in the focal area, which propagates into a SW pattern, in the neighbouring SW district, fading out at about 50 km; OVRA, near the epicenter, is an exception and moves NW-wards.

3. Immediately over the focal area, in the north-eastern district, a NE displacement is present and remains significant in the Adriatic coastal region up to a distance of about 80 km.

4. The kinematics of the stations appear to be linear with a good approximation and, in particular, the velocities seem to continue with no significant change across the event epoch; few exceptions are present in the stations near the main shock; small relaxations are visible but deeper analyses will be possible only with longer time series.

Basically, our results confirm the main shock displacements obtained by other groups and quoted in the references: the complete time series and the graphs of all the stations are freely available on line.

REFERENCES

Altamimi Z., Collilieux X., Legrand J., Garayt B. and Boucher C.; 2007: *ITRF2005: a new release of the International Terrestrial Reference Frame based on time series of station positions and Earth Orientation Parameters*. J. Geophys. Res., **112**, B09401, doi:10.1029/2007JB00494.

Anzidei M., Boschi E., Cannelli V., Devoti R., Esposito A., Galvani A., Melini D., Pietrantonio G., Riguzzi F., Sepe V. and Serpelloni E.; 2009: *Coseismic deformation of the destructive April 6, 2009 L'Aquila earthquake (central Italy) from GPS data*. Geophys. Res. Lett., **36**, L17307.

Atzori S., Hunstad I., Chini M., Salvi S., Tolomei C., Bignami C., Stramondo S., Trasatti E., Antonioli A. and Boschi E.; 2009: *Finite fault inversion of DinSAR coseismic displacement of the 2009 L'Aquila earthquake (central Italy)*. Geophys. Res. Lett., **36**, L15305.

Avallone A., Selvaggi G., D'Anastasio E., D'Agostino N., Pietrantonio G., Riguzzi F., Serpelloni E., Anzidei M., Casula G., Cecere G., D'Ambrosio C., De Martino P., Devoti R., Falco L., Mattia M., Rossi M., Obrizzo F., Tammaro U. and Zarrilli L.; 2010: *The RING network: improvements to a GPS velocity field in the central Mediterranean*. Annales of Geophysics, **53**, 39-64, doi:10.4402/ag-4549.

Barzaghi R., Borghi A., Crespi M., Pietrantonio G. and Riguzzi F.; 2004: *GPS Permanent network solution: the impact of temporal correlations*. In: V Hotine-Marussi Symposium on Mathematical Geodesy, International Association of Geodesy Symposia, vol. 127, Springer.

Benciolini B., Biagi L., Crespi M., Manzino A. and Roggero M.; 2008: *Reference frames for GNSS positioning services: some problems and proposals*. J. Appl. Geodesy, **2**, 53-62.

Biagi L. and Dermanis A.; 2006: *The treatment of time continuous GPS observations for the determination of regional deformation parameters*. In: ISDGM Proceedings, IAG Symposia, Springer-Verlag. 131, pp. 83-94.

Biagi L., Caldera S., Dominici D. and Sansò F.; 2010: *Detailed report relevant to the paper The L'Aquila 2009 event: the GPS displacements*. http://geomatica.como.polimi.it/prin/2008/.

Blewitt G. and Lavallée D.: 2002: *Effects of annual signals on geodetic velocity*. J. Geophys. Res., **107**, 2145-2155.

Cheloni D., D'Agostino N., D'Anastasio E., Avallone A., Mantenuto S., Giuliani R., Mattone M., Calcaterra S., Gambino P., Dominici D., Radicioni F. and Fastellini G.; 2010: *Coseismic and initial post seismic slip of the 2009 M_w 6.3 L'Aquila earthquake, Italy, from GPS measurements*. Geophys. J. Int., **181**, 1539-1546.

Dach R., Hugentobler U., Fridez P. and Meindl M.; 2007: *Bernese GPS Software Version 5.0*. Astronomical Institute, University of Berne.

D'Agostino N., Avallone A., Cheloni D., D'Anastasio E., Mantenuto S. and Selvaggi G.; 2008: *Active tectonics of the Adriatic region from GPS and earthquake slip vectors*. J. Geophys. Res., **113**, B12413, doi:10.1029/2008JB005860.

Devoti R., Riguzzi F., Cuffaro M. and Doglioni C.; 2008: N*ew GPS constraints on the kinematics of the Apennines subductions*. Earth Planet Sci. Lett., **273**, 163-274.

EMERGEO Working Group; 2009: *Field geological survey in the epicentral area of the Abruzzi (central Italy) seismic sequence of April 6th, 2009*. Quaderni di Geofisica, vol. 70, Ist. Naz. di Geofis. e Vulcanol, 79 pp.

Ferland R.; 2006: *IGSMail 5447.* http://igscb.jpl.nasa.gov/mail/igsmail/.

Ferland R., Gendt G. and Schone T.; 2004: *IGS reference frame maintenance.* Proceedings of IGS: Celebrating a decade of the International GPS Service, Berne, March 1-5, 2004, AIUB, Berne.

Ferretti A., Prati C. and Rocca F.; 2001: *Permanent scatterers in SAR interferometry.* IEEE T. Geoscience Remote, **39**, 8-20.

Hanssen R.; 2001: *Radar Interferometry*. Kluwer Academic Publishers, Dordrecht, The Nederlands, 328 pp.

INGV; 2009: *The L'Aquila seismic sequence.* Ist. Naz. di Geofisica e Vulcanologia, Rome. //portale.ingv.it/.

Koch K.R.; 1987: *Parameter estimation and hypothesis testing in linear models*. Springer Verlag.

Kouba J.; 2003: *A guide to using International GPS Service (IGS) products*. ftp://igscb.jpl.nasa.gov/igscb/resource/pubs/GuidetoUsingIGSProducts.pdf.

Okada Y.; 1985: *Surface deformation due to shear and tensile faults a a half space*. Bull. Seism. Soc. Am., **75**, 1135-1154.

Ray J., Altamimi Z., Collilieux X. and Van Dam T.; 2008: *Anomalous harmonics in the spectra of GPS position estimates*. GPS Solutions, **12**, 55–64.

Serpelloni E., Anzidei M., Baldi P., Casula G. and Galvani A.; 2005: *Crustal velocity and strain-rate fields in Italy and surrounding regions: new results from the analysis of permanent and non-permanent GPS networks*. Geophys. J. Int., **161**, 861-880.

Vespe F., Bianco G., Fermi M., Ferraro C., Nardi A. and Sciarretta C.; 2000: *The Italian Fiducial network: services and products*. J. Geodynamics, **30**, 327-336.

Corresponding author: Ludovico Biagi
                          Politecnico di Milano - DIIAR
                          c/o Polo Regionale di Como
                          Via Valleggio 11, 22100 Como, Italy
                          Phone: +39 031 3327562; fax: +39 031 3327519; e-mail: ludovico.biagi@polimi.it